Available online at www.sciencedirect.com
ScienceDirect
Ceramics International 37 (2011) 2117–2125
CERAMICS INTERNATIONAL
www.elsevier.com/locate/ceramint

Ibuprofen release from porous hydroxyapatite tablets

Mualla Öner *, Erman Yetiz, Esin Ay, Umut Uysal

Yıldız Technical University, Chemical Engineering Department, Davutpasa Campus, 34210 Istanbul, Turkey

Received 24 January 2010; received in revised form 8 January 2011; accepted 27 February 2011
Available online 8 April 2011

Abstract

The present study investigated drug release profiles from porous hydroxyapatite [$Ca_5(PO_4)_3OH$, HAP] tablets. HAP tablets prepared synthetically and porous structure was generated via microemulsion after sintering at 700 °C. The influence of tablet's microemulsion concentration on drug release profiles from sintered porous tablets was investigated by using ibuprofen ($C_{13}H_{18}O_2$) as model drug.

A numerical approach based on Fick's second diffusion law was used to investigate drug release kinetics from porous HAP tablets. Via this equation, diffusion coefficients were calculated for each tablet and compared. Drug release from the tablets was influenced by the porosity and tortuosity of the porous network. The drug release from porous HAP tablets was increased by microemulsion concentration. It is possible to obtain HAP based drug delivery system which has different drug release behavior by controlling microemulsion concentration in tablets before sintering.

Keywords: E. Biomedical applications; Hydroxyapatite; Drug release; Ibuprofen

1. Introduction

During the past decade, a lot of efforts have been made to develop novel drug delivery systems. A large number of systems have been employed as various drug delivery systems, such as biodegradable polymers [1], hydroxyapatite [2–6], calcium phosphate cement (CFC) [7,8], xerogels [9], hydrogels [10,11], and mesoporous silica [12,13].

Ceramic-based systems have caused enhanced interest with particular attention focused on the use of hydroxyapatite as a ceramic constituent of the system. Ceramics are biocompatible, resorbable, and porous, attempts have been made to use them as drug delivery systems. Bajpai and Benghuzzi [14] initiated studies on ceramic drug delivery by the introduction of alumina calcium phosphorous oxide ceramic capsules. Bioactive hydroxyapatite (HAP) ceramic granules have been used clinically as substitute for auto grafts, for filling bone defects [15]. Study and development of biomaterials for bone filling and replacement is one of the most important fields in orthopedic surgery. Some bioactive materials, such as hydroxyapatite, bioactive glasses, and bioceramics, could spontaneously bond to living bone in the body without fibrous tissue forming around them [16–18]. These materials could facilitate integration of osseous tissue with the implant, promoting the bone regeneration and successful cure of the osseous tissue. However, the risk of bone infection is a serious trouble associated with bone filling and replacement [19–22].

The synthesis of hydroxyapatite has been a major subject for scientists over the years since it is one of the most attractive compounds in an interdisciplinary field of sciences involving chemistry, biology, medicine, geology and engineering [23–25]. In recent years, the results of studies on hydroxyapatite (HAP) and tricalcium phosphate (TCP) as drug carriers for antibiotics [26], cytostatics [27], acetylsalicylic acid [28], indomethacin [29], hormones [30] have gained a substantial interest. Calcium phosphate drug carriers can be employed as cements or in the form of porous ceramics. The properties that make HAP superior as a biomaterial in contrast to the metals or bioinert ceramics are absence of toxicity, biocompability with hard and soft tissues and bioactivity, meaning that it will support tissue ingrowth. Using HAP is advantages because it is noninflammatory and causes no immunological, foreign body, or irritating response.

One of the most widely used non-steroidal analgesic and an antiinflammatory drug to treat bone diseases is ibuprofen (IBU) [31]. It has been extensively studied as model drug for sustained and controlled drug delivery because of its short biological half-

* Corresponding author. Tel.: +90 212 383 4726–4740; fax: +90 212 383 4725.
E-mail address: oner@yildiz.edu.tr (M. Öner).

0272-8842/$36.00
doi:10.1016/j.ceramint.2011.02.021

life (2 h), good pharmacological activity and the suitable molecule size of about 1.0–0.6 nm [31–33]. Therefore, ibuprofen has been frequently employed as a model drug on the purpose of sustained/controlled release.

In this work we present a facile way to produce hydroxyapatite (HAP) crystals by wet chemical synthesis in the presence of microemulsion under controlled temperature, pH, and atmospheric conditions. The obtained crystals were used to produce tablets by direct compression of HAP followed by removal of the organic content via heat treatment to create porous matrices. The drug storage/release kinetic in synthetic body fluid (SBF) was investigated on this system using ibuprofen (IBU) as a model drug.

2. Materials and methods

2.1. Preparation of seed

Calcium chloride, potassium hydroxide and dipotassium hydrogen phosphate (reagent grade) were from J.T. Baker. Ciba Glaskol LS 16 specialty resin was used to produce porous HAP. It is an aqueous microemulsion based on styrene-acrylic copolymers. Two hundred fifty milliliters of 0.50 mol/L $CaCl_2$ and 0.10 mol/L KOH to adjust the pH at 9.5 were added to the reaction vessel, which was thermostated at 70 °C. This solution was mixed with 0.30 mol/L dipotassium hydrogen phosphate solution, which was added dropwise over a period of 2 h. During the precipitation process, the pH was kept constant between 9.0 and 9.5 by small additions of KOH solution. The reactor was stirred with a magnetic stirrer at approximately 550 rpm. The presaturated nitrogen gas was introduced into the stirred solution during reaction to ensure a CO_2 free atmosphere. In experiments where microemulsion was used for obtaining hydroxyapatite crystals a similar procedure was followed and freshly prepared polymer solutions were normally added to the phosphate solution at concentration of 1–15 g/L. The obtained crystals were dried at 60 °C in a vacuum and then used to produce tablets by pressing at 3.5 tons for 10 s. The cylindrical tablets with a diameter of ∼13 mm were obtained. The pressed tablets were sintered in a chamber furnace at 700 °C during 3 h. Calcination serves a dual purpose, removing organic material to create a porous structure and crystallizing of HAP.

Sample codes and amount of microemulsion used to manufacture porous tablets are shown in Table 1.

2.2. Drug loading

Ibuprofen (IBU) was used as the model drug. Porous tablet was added into 25 ml of hexane solution with an ibuprofen concentration of 40 g/L at room temperature and soaked for 24 h with stirring in a vial which was sealed to prevent the evaporation of hexane. The IBU loaded tablet was separated and then kept at in a drying oven at 50 °C for 24 h.

Table 1
Samples designation.

Sample codes	Microemulsion (g/L)
Sp1	1
Sp2	2
Sp3	5
Sp4	15

2.3. Drug release

Ibuprofen release tests from different HAP tablets were performed at 20 °C and 37 °C in 100 ml synthetic body fluid (Merck standard SBF, pH 7.4). HAP tablets immersed in 100 ml dissolution medium in a glass bottle with paddle speed of 250 rpm. Samples were collected at different time points. Ibuprofen concentration in the sampled release fluid was measured on an UV/vis spectrometer (Specord 50 Analytik Jena UVS) at wavelength of 264 nm. All experiments were done in triplicate and mean values were reported. The reproducibility of the experimental results was ∼2–6%.

2.4. Characterization

X-ray diffraction analysis of the HAP samples was carried out by means Phillips Panalytical X'ert Pro powder diffractometer operating with Cu Kα radiation in operating at 40 mA and 40 kV. The 2θ range was from 10° to 60° at scan rate of $0.020^\circ\ \text{step}^{-1}$. Purity of the seed samples was also tested by FTIR (Perkin Elmer) spectral analysis. The mercury porosimetry (Micromeritics AutoPore IV 9500) was used to determine average pore diameter, porosity and tortuosity of tablets. The porosity of the tablets was analyzed by scanning electron microscopy (JEOL-FEG-SEM).

2.5. Mathematical analysis

The mathematical theories were used to analyze the experimentally measured in vitro drug release kinetics and to determine the apparent diffusion coefficient of ibuprofen within the HAP tablets. The solution model is based on Fick's second law of diffusion [34], considering axial as well as radial mass transfer in a cylinder was used to quantitatively describe the experimentally measured drug release profiles (Eq. (1)):

$$\frac{\partial c}{\partial t} = \frac{1}{r}\left\{\frac{\partial}{\partial r}\left(rD\frac{\partial c}{\partial r}\right) + \frac{\partial}{\partial \theta}\left(\frac{D}{r}\frac{\partial c}{\partial \theta}\right) + \frac{\partial}{\partial z}\left(rD\frac{\partial c}{\partial z}\right)\right\} \quad (1)$$

At this equation c is the drug concentration, t is the time, r and z are the radial and axial coordinates respectively and θ is the angle perpendicular to the r–z-plane, and D is the apparent diffusion coefficient of the drug within the porous tablet.

Taking into account the following initial and boundary conditions [35]:

(i) Perfect sink conditions are maintained throughout the experiment.
(ii) The pellets are cylindrical in shape.
(iii) The diffusion coefficient of ibuprofen is constant.
(iv) The drug is initially uniformly distributed throughout the pellets before exposure to the release medium ($t = 0$).

Using infinite series of exponential functions this partial differential equation can be solved considering the respective initial and boundary conditions [35]:

$$\frac{M_t}{M_\infty} = 1 - \frac{32}{\pi^2}\sum_{n=1}^{n=\infty}\left[\frac{1}{(q_n)^2}\exp\left[-\frac{(q_n)^2}{r^2}Dt\right]\right] \times \sum_{p=0}^{p=\infty}\left[\frac{1}{(2p+1)^2}\exp\left[Dt\frac{-(2p+1)^2\pi^2}{H^2}\right]\right] \quad (2)$$

where M_t and M_∞ represent the absolute cumulative amounts of drug released at time t and infinite time (in this work where the drug concentration was stabilized), respectively, q_n are the roots of the Bessel function of the first kind of zero order ($J_0(q_n) = 0$), and r and H denote the radius and height of the cylinder.

3. Results and discussion

3.1. Characterization of porous tablets

Fig. 1a and b summarizes the XRD patterns of HAP heated at the temperature of 700 °C. XRD spectra of all samples have shown peaks characteristic for HAP. The crystals were identified as hydroxyapatite by XRD (Fig. 1a and b) and compared with that of the ASTM (09-0432) standards. The principal diffraction peaks of HAP appears at 2θ values of 25.9° for reflection (0 0 2), at 31.9° (triplet) for reflections (2 1 1), (1 1 2) and (3 0 0), and at 34° for reflection (2 0 0). All intensity peaks of the XRD patterns of the HAP powders produced were exactly matched with the structural data of the HAP described in ASTM standards, although the intensities of the XRD peaks were varied with the reaction conditions.

The FTIR spectra for sintered Sp4, IBU, IBU loaded Sp4 and Sp4 after dissolution of the IBU are displayed in Fig. 2a–d respectively. FT-IR spectra of the samples also showed that they consisted of HAP (Fig. 2a). The group PO_4^{3-} can be attributed to the strong douplet between 1036 and 1100 cm^{-1} (antisymmetric stretching modes, υ_3), the band at 962 cm^{-1} (symmetric mode, υ_1), and the bands at 605 cm^{-1} and 570 cm^{-1} are assigned to the O–P–O bending mode υ_4 [36]. The shoulder at 3571 cm^{-1} is characteristics for stretching modes of the OH^- ions. The medium sharp peak at 632 cm^{-1} can be assigned to the O–H bending deformation mode, and indicates the presence of HAP phase. The broad band centered around at 3435 cm^{-1} and the band at 1635 cm^{-1} show the presence of water in the samples. CO_3^{2-} ions were detected in the precipitate from the peaks at 1453 cm^{-1}, 1413 cm^{-1} and 877 cm^{-1}. Fig. 2b shows that, ibuprofen possesses an intense and well defined infrared band at 1720 cm^{-1} attributed to the stretching of C=O group [37]. For the IBU-loaded tablet (Fig. 2c), the band assigned to the vibration of –COOH at 1720 cm^{-1} is obvious except for a slight decrease of intensity compared with that of IBU (Fig. 2b). Furthermore, the absorption bands assigned to the quaternary carbon atom located at 1462 cm^{-1} and 1510 cm^{-1} tertiary carbon atom at 1340 cm^{-1}, O–H bending vibration at 1416 cm^{-1}, and C–Hx bond at 2924 cm^{-1} and 2955 cm^{-1} can also be observed (Fig. 2c), confirming the successful adsorption of IBU onto the tablets and also 1039 cm^{-1} band represents that tablet has typical PO_4^{-3} bond [37]. The infrared band for IBU was not observed for Sp4 after dissolution (Fig. 2d). This results confirmed complete release of IBU from the tablet.

The pore-size of the porous tablets was examined both qualitatively by SEM and quantitatively, by mercury porosimeter. The obtained HAP tablets showed varying porosity, depending mostly on the amount of pore-creating additive. The pore size of the samples was defined according to the International Union of Pure and Applied Chemistry (IUPAC) which is stated that micropores are smaller than 2 nm in diameter, mesopores 2–50 nm and macropores larger than 50 nm. The SEM micrograph in Fig. 3a and b represents the cross-sectional view of the internal structure of the porous tablet at high magnification. SEM analysis of the studied materials revealed that microemulsion, after its complete destruction, leaves an irregularly shaped porosity with the presence of single macropores, i.e. pores of over 1–5 μm diameter (Fig. 3a and b). The macropores are visible in Sp4, while the Sp3 exhibited a less porous matrix. The larger pore size detected for tablets prepared with 15 g/L microemulsion concentration. Since it is very difficult to quantify a three dimensional porosity via two-dimensional microscopic observation, porosimeter was used to determine the entire pore size distribution. In contrast to the pore size detected by SEM the pore size distribution determined via mercury porosimetry was

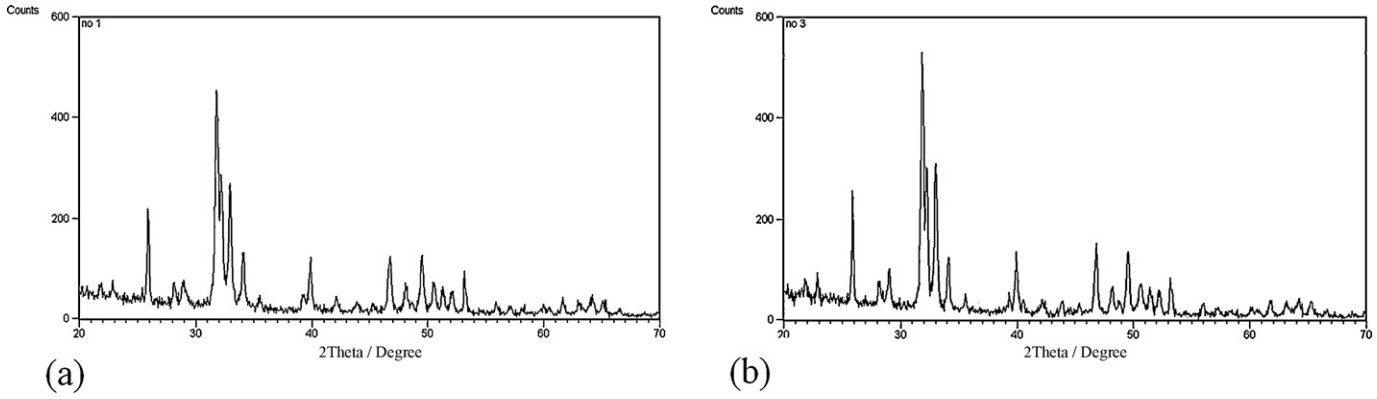

Fig. 1. XRD pattern of HAP tablets: (a) in the absence of microemulsion and (b) in the presence of microemulsion.

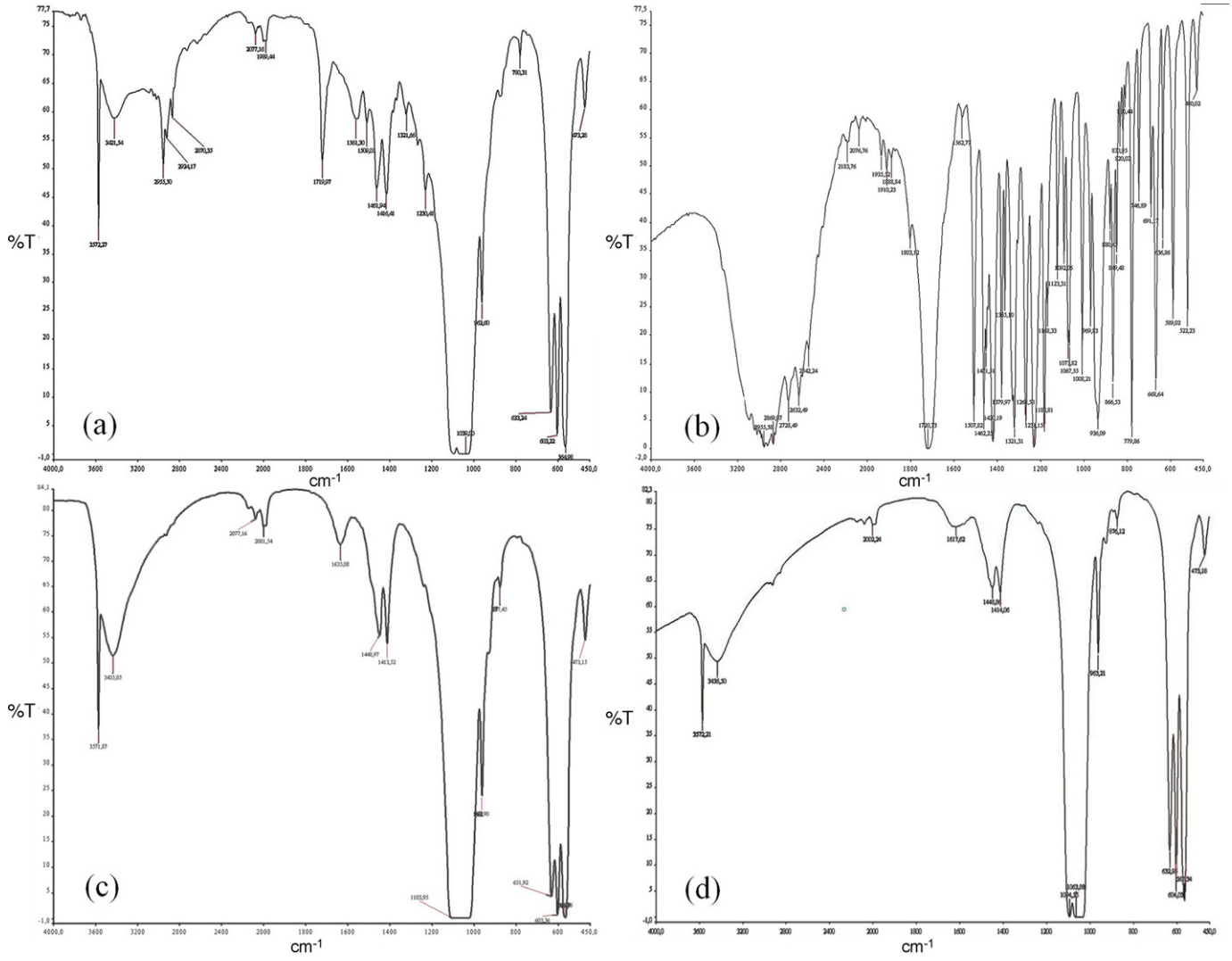

Fig. 2. FTIR spectra of Sp4 (a), IBU (b), IBU–Sp4 after adsorption (c) and IBU–Sp4 after dissolution (d).

much smaller. The fraction of large holes did not reveal by porosimetric analysis. However, comparison between both methods is difficult since their approach is different. In order to be able to compare and discuss the porous structure of investigated samples the distribution of pore size is given in Fig. 4a and b. Table 2 contains the data for tablets in terms of their porosity, total intrusion volume and average pore diameter. Porosity of the sintered tablets depended on the

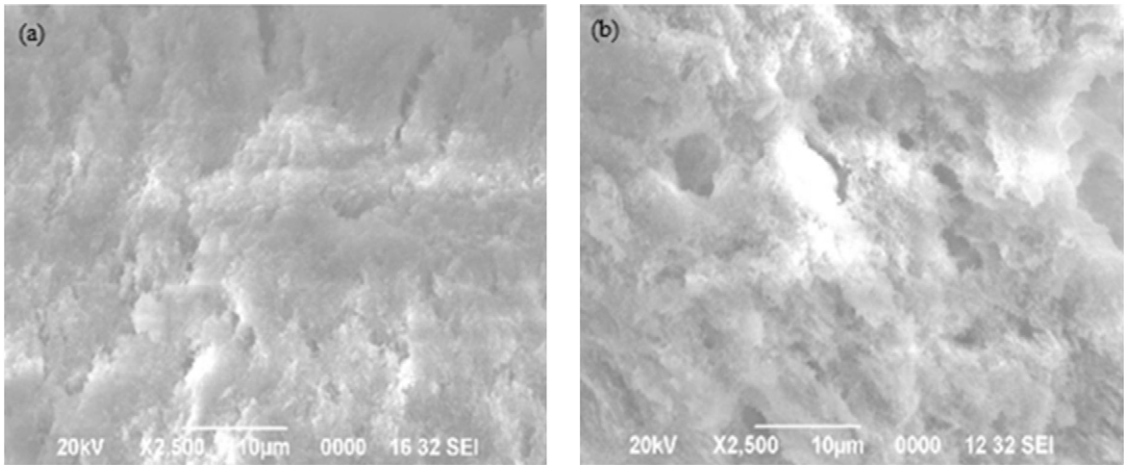

Fig. 3. SEM photographs of Sp3 (a) and Sp4 (b).

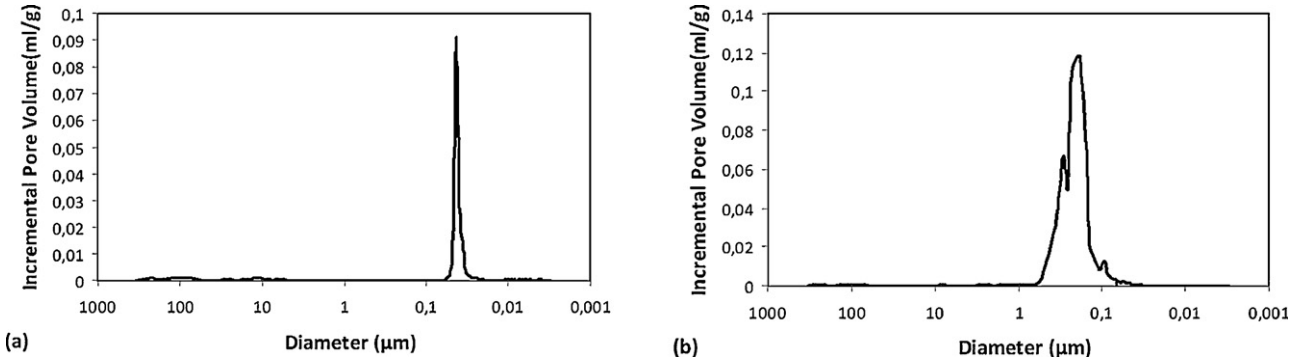

Fig. 4. Unimodal distribution of pores in control sample (a) and bimodal distribution of pores in sample Sp4 (b).

Table 2
Physical properties of HAP tablets.

Sample designation	Total ıntrusion volume (mL/g)	Average pore diameter (nm)	Porosity (%)	Tortuosity
Control	0.28	35.2	46.4	32.63
Sp1	0.28	42.7	45.0	30.98
Sp2	0.30	35.4	47.3	24.60
Sp3	0.40	60.1	54.7	22.00
Sp4	0.59	146.4	64.6	18.80

amount of pore former. Increasing the amount of pore forming agent resulted in a higher porosity as the inorganic phase was removed during the heat treatment.

According to results given in Table 2 and Fig. 4b, the sample Sp4 has the highest pore diameter and porosity. By analyzing the histogram in Fig. 4, it can be observed that in Sp4 the occurrence of macropores is higher. Maximum in the pore diameter of about 146 nm is obtained for the tablets, which have been prepared with the use of the 15 g/L microemulsion content (Table 2). To compare, it can be noted that if pure HAP powder without sintering additives is used for drug release allows the fabrication of the low-pore-content bulk ceramic bodies (Fig. 4a). The porosity of tablets ranged from 45% to about 64%, The increase in the amount of pore-creating additive from 1 g/L to 15 g/L resulted in a nearly 30% increase in the porosity. Maximum in the porosity of about 64% is obtained for the tablets, which have been prepared with the use of the mixtures of the highest microemulsion content. The distribution of pores in tablets varied, being unimodel in the case of control and bimodel for Sp4.

3.2. Drug loading and release properties

The adsorption of ibuprofen from hexane was studied by determining adsorption isotherms for sample Sp4. In Fig. 5, the corresponding isotherm is expressed as the amount ibuprofen adsorbed per weight tablets, *n*/*w*, as a function of the equilibrium concentration of ibuprofen in hexane solution, C_{eq}. The adsorbed amount of IBU increased linearly in the range of 0–200 mmol/L of the IBU solution. It can be seen that the data for adsorptive uptake of ibuprofen from hexane by HAP show Langmuir-type isotherms. The adsorption of solutes from nonaqueous solvents on hydroxyapatite is mainly regulated by the interplay of hydrogen bonding between adsorbate, adsorbent and solvent. The main interaction sites between the ibuprofen and the hydroxyapatite surface are thought to be hydrogen bonding; that is, formation of the hydrogen bonding between the carboxyl groups of IBU with the OH groups on the surface.

In Figs. 6–9, the cumulative percentage of IBU released to SBF versus soaking time is plotted for samples of the four series obtained. In tablets, the delivery profile is very similar, showing two release stages: in the first 30–100 min the release is fast, in this period about 50% of drug content is released. After that,

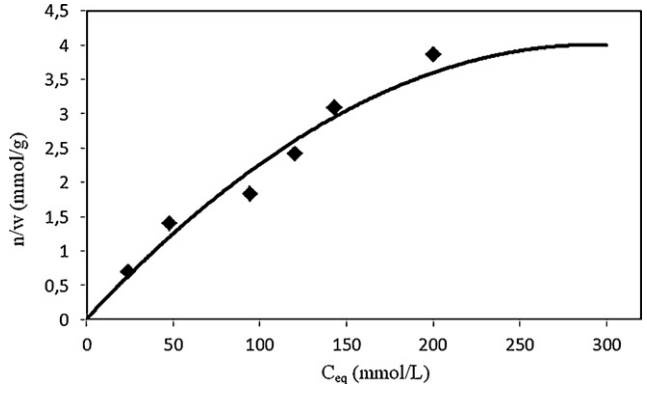

Fig. 5. The adsorption isotherms of ibuprofen in hexane solution for sample Sp4.

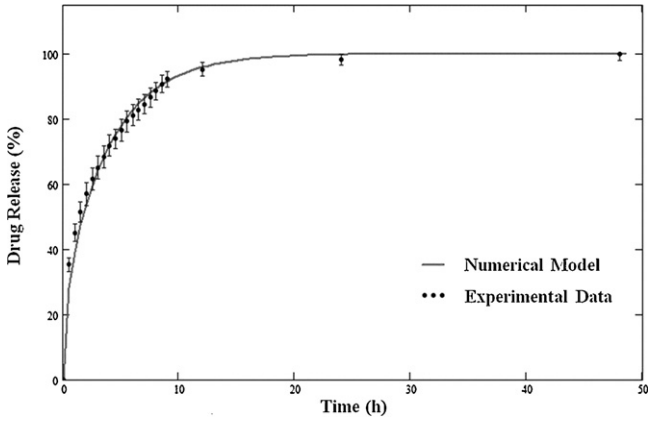

Fig. 6. Drug release from sample Sp1 at 37 °C.

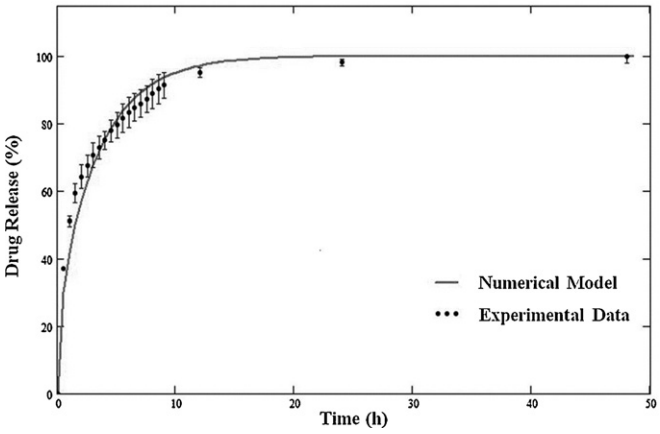

Fig. 7. Drug release from sample Sp2 at 37 °C.

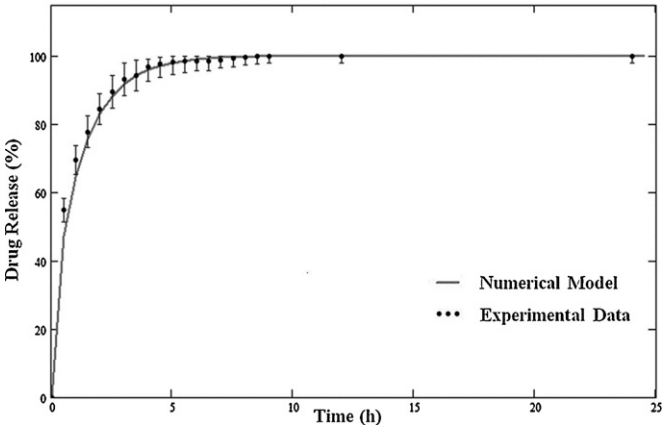

Fig. 9. Drug release from sample Sp4 at 37 °C.

between 2 and 24 h, the drug delivery rate is much lower and the tablets stopped the IBU release at 5–15 h depending on the porosity of the samples. A comparison of the curves in Figs. 6–9 shows that the increase in the release rate and its maximum value were higher in the case of tablets prepared with higher amount of pore former.

Irrespective of the type of tablets, the IBU release rate was particularly high at early time points. This is a typical behavior of diffusion-controlled drug delivery systems: at early time points, the diffusion pathways are short, resulting in steep concentration gradients (being the driving forces for diffusion) and, thus, high drug release rates. With increasing time, the length of the diffusion pathways increases, resulting in decreased drug concentration gradients and, thus, decreased drug release rates. To better understand the underlying drug release mechanisms, an analytical solution of Fick's second law of diffusion (Eq. (2)) was fitted to the experimentally determined IBU release kinetics (Figs. 6–9). This theory is based on the assumption that drug release is purely diffusion-controlled. It considers the cylindrical geometry of the tablets and the fact that perfect sink conditions are maintained throughout the experiments. Fitting an appropriate analytical solution of Fick's second law of diffusion, considering axial as well as radial mass transport in cylinders, Eq. (2), to the experimentally measured IBU release profiles obtained in SBF resulted in good agreement between theory and experiment. This indicates that drug release from these systems is primarily diffusion-controlled. Based on these calculations, the effective diffusion coefficients of IBU in the porous tablets upon exposure to SBF could be determined. Table 3 shows the computed diffusion coefficients, for tablets and Figs. 6–9 show corresponding errors at 37 °C. Note that each of the D_{eff} values calculated is representing an average diffusivity for IBU through the pore spaces of the samples. Transport through the HAP tablets is the solute transport in porous media. In this system the matrix is formed by a mesh of interlocking of crystals which create micro or even nanoporosity. The diffusion coefficient in such a system is an effective diffusion coefficient (D_{eff}), related to the diffusion coefficient of the drug through the pores filled with a solution of drug, D_i:

$$D_{eff} = \frac{D_i \varepsilon}{\tau} \quad (3)$$

where ε is the tablets porosity, τ is the tortuosity interpreted as a correction factor for the increased length of the diffusion path caused by the pore network. For example, in the case of a straight cylindrical pore, the tortuosity is 1 because the diffusion path is straight. If the pores are tilted at 45°, the tortuosity becomes $\sqrt{2}$. Therefore, it is clear that porosity and other microstructural parameters of the material play an important role in the kinetics of drug release. This dependence has been shown by Otsuka [38–40] in several works and found by other researchers [41–43], in works covering different calcium phosphate cement (CPC) formulations and different drugs. Otsuka et al. investigated drug delivery behaviour of self setting calcium phosphate cement containing aspirin as a model drug

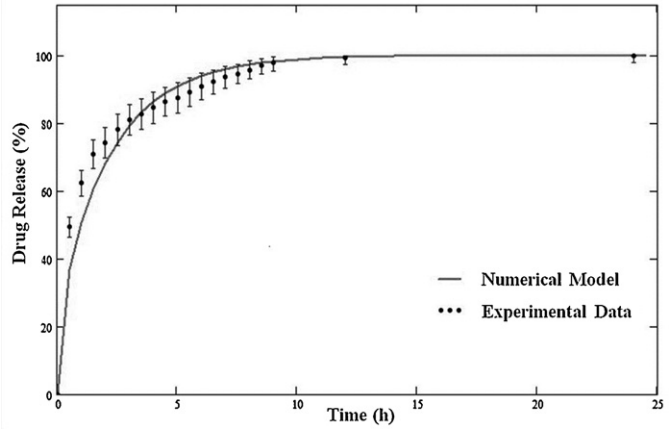

Fig. 8. Drug release from sample Sp3 at 37 °C.

Table 3
The Diffusion Coefficient (D_{eff}) of the IBU in porous tablets at 20 °C and 37 °C.

Sample designation	D_{eff} ($\times 10^7$ m^2/h) at 20 °C	D_{eff} ($\times 10^7$ m^2/h) at 37 °C
Control	0.34	1.62
Sp1	1.02	2.04
Sp2	1.10	2.32
Sp3	2.55	3.56
Sp4	5.35	6.19

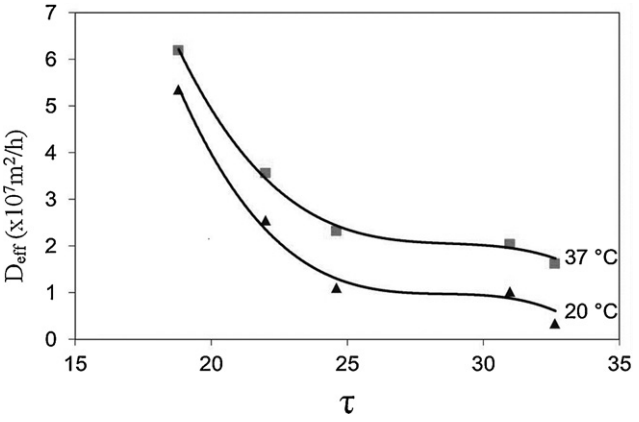

Fig. 10. The relationship between the diffusion coefficient and the tortuosity of HAP tablets.

[28]. They found that the drug release rates from the cement were controlled by the porosity and tortuosity of the cements. They also reported that the release rate from the cements decreased with increasing tortuosity. We observed similar relationship in our system. Fig. 10 shows the relationship between the effective diffusion coefficient and the tortuosity of the pores in the tablets. As the diffusion coefficient increases from 1.62×10^{-7} to 6.19×10^{-7} m^2/h, the tortuosity of the pores decreases from 32.63 to 18.8. This result suggests that tortuosity is playing an important role in drug release through the tablets.

The effective diffusion coefficients of IBU molecules were in the order of 10^{-7} m^2/h. Figs. 6–9 show that the experimental release values do not deviate significantly from the mathematical model employed in this study. The diffusion coefficients of IBU within the porous tablets increased with increasing porosity. Samples Sp3 and Sp4 have the largest observed diffusion coefficients and pore sizes. The control sample exhibits both the smallest pore space and has diffusion coefficients approaching the lowest order. From the control sample to the most porous sample Sp4, the diffusion coefficient changed from 1.62×10^{-7} to 6.19×10^{-7} m^2/h. The similar relationship was also observed by other researcher [35]. Tablets containing hydroxyapatite and a pore forming agent were manufactured by direct compression followed by sintering [35]. Aqueous drug solutions (metoprolol tartrate, riboflavin sodium phosphate) were used to investigate drug release rates. It was found that, drug release from the porous carrier was primarily diffusion controlled; the apparent drug diffusivity was depending on the pore size of the porous network. The apparent diffusion coefficients of riboflavin sodium phosphate and metoprolol tartrate in the porous tablets upon exposure to water were found $D = 1.9 \times 10^{-6}$ cm^2/s and $D = 1.2 \times 10^{-6}$ cm^2/s, respectively [35].

In all release curves, an initial burst within 100 min followed by a 5–15 h release was observed. Indeed, faster diffusion is occurring from tablets exhibiting the greater porous matrix. The initial burst may be due to release from exogenously bounded drugs on the surface of the tablets. During the loading and release process, the IBU molecules can be adsorbed onto the surface of porous materials in the impregnation process and liberated by diffusion-controlled mechanism. The initial burst was also observed by other researchers. Bioactive, luminescent and mesoporous europium-doped hydroxyapatite (Eu:HAp) was prepared as a drug delivery carrier to investigate the drug storage/release properties using ibuprofen (IBU) as a model drug [37]. The HAP crystals show a burst release of about 50% within 1 h followed by the relatively slow release and complete release after 24 h [37]. Cylindrical hydroxyapatitic grafts at two different degree of porosity (60% and 40%) were tested as controlled drug delivery devices in order to evaluate the fundamental parameters which control release kinetics of ibuprofen-lysine and hydrocortisone Na-succinate [44]. The burst release was observed within 40 min. After the first 40 min, hydrocortisone Na-succinate release kinetics results slower than ibuprofen lysine [44]. This behaviour was explained due to the difficulty for the more sterically hindered molecules to move throughout microporosity [44]. Vallet Regi et al. investigated potential property of MCM-41 mesoporous molecular sieves for controlled drug delivery systems [45,46]. For this purpose IBU was used as a model drug. It was found that the drug release profiles could be controlled by tailoring the morphologies of mesoporous silica carriers. All the drug incorporated into the MCM-41 matrix was released to the solution after 3-days by optimizing the method of IBU loading [45,46]. The ibuprofen (IBU)-loaded poly(3-hydroxybutyrate-*co*-3-hydroxyvalerate) (PHBV) microparticles were fabricated by conventional solvent evaporation [47]. The half release time was found from 15 to 62 h depending on the size of microparticles [47].

The OH^- groups on the surface should be the reaction sites to form hydrogen bonding with the carboxyl group of IBU when IBU is adsorbed on the surface. It is difficult to exclude some materials that may have been attached to the outer surface. The typical 50% initial release burst may be related to the dissolution of this externally attached matter. The initial drug burst associated with quick dissolution of externally attached drug was larger for sample Sp3 and Sp4. Burst release can be examined two different perspectives: positive and negative [48]. Positive perspective focuses on situations in which rapid release of high drug concentration is desirable such as at the beginning of wound treatment. In these cases, an initial burst provides the patient with immediate relief followed by a prolonged release to improve gradual healing. The negative aspects of burst release are economic and therapeutic waste of drug [48].

3.2.1. Effect of temperature on drug release rate

Furthermore, a series of drug release experiments were performed at 20 °C in order to see temperature effect on release rate. Fig. 11 shows the drug release profiles from the tablets in pH 7.4 at 20 °C. The plotted graphs revealed that all the samples showed same type drug-release patterns. The ibuprofen release rate rapidly increased, reaching a maximum 2–4 h after the beginning of the experiment. After that, the released substance content in the SBF reaches a plateau.

The calculated and experimental IBU release profile is plotted in Fig. 11 which shows that decreasing the diffusion

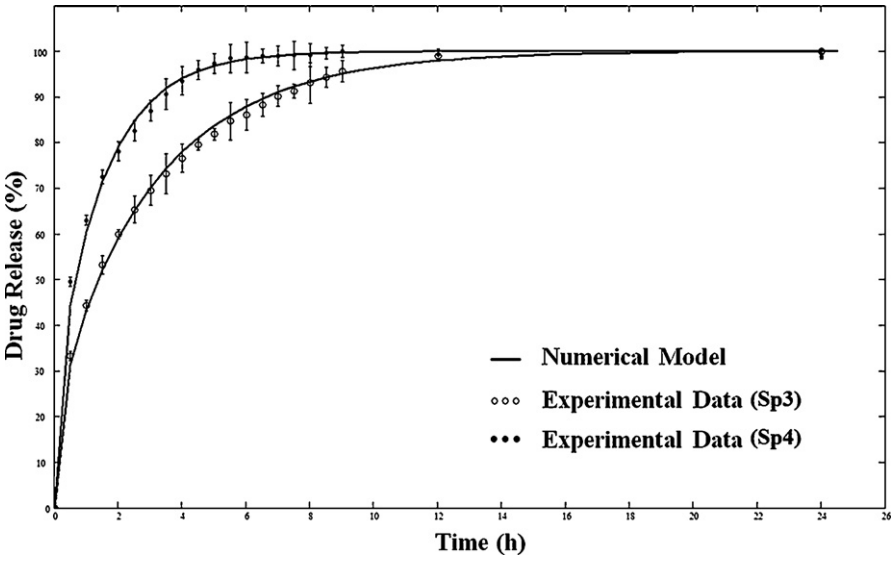

Fig. 11. Drug release from sample Sp3 and Sp4 at 20 °C.

coefficient obviously results in lower rate of release as would be expected. The diffusion coefficients calculated for IBU molecules within these tablets are presented in Table 3. The experimental results showed a trend of decreasing D_{eff} with lowering temperature. Hence, lower temperature restricted the free movement of IBU molecules. These results suggest that the diffusion of IBU molecules through the porous network can be controlled by temperature.

It is well known that increase in temperature results in an increase in molecular diffusion rate. There is barrier to diffusion created by neighboring atoms. This barrier should be relocated in order to allow diffusion atoms to pass. Temperature is a measure of molecular motion. Thus atomic vibrations created by temperature assist to diffusion. Lin et al. [49] tested drug delivery system involving diffusion of the drugs and observed in significant increase in diffusion rate at 37 °C compared to those obtained at 24 °C. It was reported that release rate increased by a factor of 3, 2 and 5 for different drugs.

4. Conclusion

The aim of this work was to elucidate the underlying drug release mechanisms from HAP tablets, using IBU as model drug. The effects of different formulations and processing parameters on the resulting drug release kinetics in SBF and pH 7.4 were studied and the obtained results were analyzed using adequate mathematical models in order to get further insight into the underlying mass transport mechanisms. The micro-emulsion content of the tablet was found to strongly affect the underlying drug release mechanisms. Drug release from tablets was primarily controlled by diffusion-controlled drug release rate. The effective diffusion coefficient is depending on the porosity and tortuosity of the porous tablets. The burst release seen in the dissolution profiles was attributed to the presence of drug on the surface of the tablet, while sustained release was attributed principally to the location of drug within the pores. The effects of the pore size of tablets prepared on the resulting drug release kinetics could be quantitatively predicted using an analytical solution of Fick's second law of diffusion. This result suggests the possibility of predicting the drug delivery from HAP tablets in different situations.

In summary, a simple one-step synthesis route for making a porous hydroxyapatite tablets is proposed. This material exhibits porous crystalline structure, which is suitable for drug (IBU) release as a drug carrier. This system demonstrates a potential application in the fields of drug delivery and disease therapy based on its bioactive and porous properties.

Acknowledgements

We appreciate the support of YTUAF (Project No: 27-07-01-02); DPT (Project No: 24-DPT-07-04-01 and Project No: 25-DPT-07-04-01) for funding this work.

References

[1] K.E. Uhrich, S.M. Cannizzaro, R.S. Langer, K.M. Shakesheff, Polymeric systems for controlled drug release, Chem. Rev. 99 (11) (1999) 3181–3198.
[2] M. Itokazu, W. Yang, T. Aoki, A. Ohara, N. Kato, Synthesis of antibiotic-loaded interporous hydroxyapatite blocks by vacuum method and in vitro drug release testing, Biomaterials 19 (7–9) (1998) 817–819.
[3] A. Almirall, G. Larrec, J.A.A. Delgado, Fabrication of low temperature macroporous hydroxyapatite scaffolds by foaming and hydrolysis of an alpha-TCP paste, Biomaterials 25 (17) (2004) 3671–3680.
[4] J.E. Barralet, K.J. Lilley, L.M. Grover, D.F. Farrar, C. Ansell, U. Gbureck, Cements from nanocrystalline hydroxyapatite, J. Mater. Sci. Mater. Med. 15 (4) (2004) 407–411.
[5] V. Komlev, S. Barinov, E. Koplik, A method to fabricate porous spherical hydroxyapatite granules intended for time-controlled drug release, Biomaterials 23 (16) (2002) 3449–3454.
[6] M.A. Rauschmann, T.A. Wichelhaus, V. Stirnal, E. Dingeldein, L. Zichner, R. Schnettler, A. Volker, Nanocrystalline hydroxyapatite and calcium sulphate as biodegradable composite carrier material for local delivery of antibiotics in bone infections, Biomaterials 26 (15) (2005) 2677–2684.

[7] R.P. del Real, J.G.C. Wolke, M.A. Vallet-Regi, New method to produce macropores in calcium–phosphate cements, Biomaterials 23 (17) (2002) 3673–3680.
[8] M. Bohner, Calcium orthophosphates in medicine: from ceramics to calcium–phosphate cements, Injury 31 (4) (2009) 37–47.
[9] H.H. Yang, Q.Z. Zhu, H.Y. Qu, X.L. Chen, M.T. Din, J.G. Xu, Flow injection fluorescence immunoassay for gentamicin using sol–gel derived mesoporous biomaterial, Anal. Biochem. 308 (1) (2002) 71–76.
[10] P. Caliceti, S. Salmaso, A. Lante, M. Yoshida, R. Katakai, F. Martellini, L.H.I. Mei, M. Carenza, Controlled release of biomolecules from temperature-sensitive hydrogels prepared by radiation polymerization, J. Controlled Release 75 (1–2) (2001) 173–181.
[11] M. Changez, K. Burugapalli, V. Koul, V. Choudhary, The effect of composition of poly (acrylic acid)–gelatin hydrogel on gentamicin sulphate release: in vitro, Biomaterials 24 (4) (2003) 527–536.
[12] C.Y. Lai, B.G. Trewyn, D.M. Jeftinija, K. Jeftinija, S. Xu, S. Jeftinija, V.S.Y. Lin, A mesoporous silica nanosphere-based carrier system with chemically removable CdS nanoparticle caps for stimuli-responsive controlled release of neurotransmitters and drug molecules, J. Am. Chem. Soc. 125 (15) (2003) 4451–4459.
[13] F.Y. Qu, G.S. Zhu, H.M. Lin, J.Y. Sun, D.L. Zhang, S.G. Li, S.L. Qui, A controlled release of ibuprofen by systematically tailoring the morphology of mesoporous silica materials, J. Solid State Chem. 179 (7) (2006) 2027–2035.
[14] P.K. Bajpai, H.A. Benghuzzi, Ceramic systems for long-term delivery of chemicals and biologicals, J. Biomed. Mater. Res. 22 (12) (1988) 1245–1266.
[15] O. Oonishi, Orthopaedic application of hydroxyapatite, Biomaterial 12 (2) (1991) 171–178.
[16] L.L. Hench, R.J. Splinter, W.C. Allen, T.K. Greenlee, Bonding mechanisms at the interface of ceramic prosthetic materials, J. Biomed. Mater. Res. 2 (1) (1972) 117–141.
[17] L.L. Hench, Bioceramics: from concept to clinic, J. Am. Ceram. Soc. 74 (7) (1991) 1487–1510.
[18] M. Vallet-Regi, C.V. Ragel, A.J. Salinas, Glasses with application, Eur. J. Inorg. Chem. 2003 (6) (2003) 1029–1042.
[19] T. Nakamura, T. Kokuba, Quantitative study on osteoconduction of apatite-wollastonite containing glass ceramic granules, hydroxyapatite granules, and alumina granules, Biomaterials 11 (4) (1990) 265–270.
[20] P.E Ochsner, S. Hailemariam, Histology of osteosynthesis associated bone infection, Injury 37 (2) (2006) S49–S58.
[21] B.M. Tracy, R.H. Doremus, Direct electron microscopy studies of the bone hydroxylapatite interface, J. Biomed. Mater. Res. 18 (7) (1984) 719–726.
[22] F. Korkusuz, A. Uchida, Y. Shinto, N. Araki, K. Inoue, K. Ono, Experimental implant-related osteomyelitis treated by antibiotic-calcium hydroxyapatite ceramic composites, J. Bone Joint Surg.—Br. 75 (1) (1993) 111–114.
[23] O. Dogan, M. Oner, The influence of polymer architecture on nanosized hydroxyapatite precipitation, J. Nanosci. Nanotechnol. 8 (2) (2008) 667–674.
[24] O. Dogan, M. Oner, Biomimetic mineralization of hydroxyapatite crystals on the copolymers of vinylphosphonic acid and 4-vinilyimidazole, Langmuir 22 (23) (2006) 9671–9675.
[25] M. Oner, O. Dogan, Inhibitory effect of polyelectrolytes on crystallization kinetics of hydroxyapatite, Prog. Cryst. Growth Charact. Mater. 50 (1–3) (2005) 39–51.
[26] D. Yu, J. Wong, Y. Matsuda, J.L. Fox, W.I. Higuchi, M. Otsuka, Self-setting hydroxyapatite cement: a novel skeletal drug-delivery system for antibiotics, J. Pharm. Sci. 81 (6) (1992) 529–532.
[27] M. Otsuka, Y. Matsuda, Y. Suwa, J.L. Fox, W.I. Higuchi, A novel skeletal drug delivery system using a self-setting calcium phosphate cement. 5. Drug release behavior from a heterogenous drug-loaded cement containing an anticancer drug, J. Pharm. Sci. 83 (11) (1994) 1565–1568.
[28] M. Otsuka, Y. Matsuda, Y. Suwa, J.L. Fox, W.I. Higuchi, A novel skeletal drug delivery system using a self-setting calcium phosphate cement. 4. Effects of the mixing solution volume on the drug-release rate of heterogeneous aspirin-loaded cement, J. Pharm. Sci. 83 (2) (1994) 259–263.
[29] M. Otsuka, Y. Nakahigashi, Y. Matsuda, J.L. Fox, W.I. Higuchi, A novel skeletal drug-delivery system using self-setting calcium phosphate cement. 7. Effect of biological factor on indomethacin release from the cement loaded on bovine bone, J. Pharm. Sci. 83 (11) (1994) 1569–1573.
[30] M. Otsuka, Y. Matsuda, Y. Suwa, J.L. Fox, W.I. Higuchi, A novel skeletal drug-delivery system using self-setting calcium phosphatecement. 3. Physicochemical properties and drug release rate of bovine insulin and bovine albumin, J. Pharm. Sci. 83 (2) (1994) 255–258.
[31] S. Ladron de Guevara-Fernandez, C.V. Ragel, M. Vallet-Regi, Bioactive glass-polymer materials for controlled release of ibuprofen, Biomaterials 24 (22) (2003) 4037–4043.
[32] A. Krajewski, A. Ravaglioli, E. Roncari, P. Pinasco, L. Montari, Porous ceramic bodies for drug delivery, J. Mater. Sci. Mater. Med. 11 (12) (2000) 763.
[33] N. Ahola, J. Rich, T. Karjalainen, J. Seppälä, Release of ibuprofen from poly(ε-caprolactone-co-D,L-lactide) and simulation of the release, J. Appl. Polym. Sci. 88 (5) (2003) 1279.
[34] J. Crank, The Mathematics of Diffusion, 2nd ed., Oxford University Press, Oxford, 1975.
[35] A. Cosijns, C. Vervaet, J. Luyten, S. Mullen, F. Siepman, L. Van Hoorebek, B. Masschaele, V. Cnuddan, J.P. Remon, Porous hydroxyapatite tablets as carriers for low-dosed drugs, Eur. J. Pharm. Biopharm. 67 (2) (2007) 498–550.
[36] A. Slosarczyk, Z. Paszkiewicz, C. Paluszkiewicz, FTIR and XRD evaluation of carbonated hydroxyapatite powders synthesized by wet methods, J. Mol. Struct. 744–747 (2005) 657–661.
[37] P. Yang, Z. Quan, C. Li, X. Kang, H. Lian, J. Lin, Bioactive, luminescent and mesoporous europium-doped hydroxyapatite as a drug carrier, Biomaterials 29 (32) (2008) 4341–4347.
[38] M Otsuka, Y. Nakahigashi, Y. Matsuda, J.L. Fox, W.I. Higuchi, Y. Sugiyama, Effect of geometrical cement size on in vitro indomethacin release from self-setting apatite cement, J. Controlled Release 52 (3) (1998) 281–289.
[39] M. Otsuka, Y. Nakahigashi, Y. Matsuda, J.L. Fox, W.I. Higuchi, Y. Sugiyama, A novel skeletal drug delivery system using self-setting calcium phosphate cement VIII: the relationship between in vitro and in vivo drug release from indomethacin-containing cement, J. Controlled Release 43 (2–3) (1997) 115–122.
[40] M. Otsuka, Y. Matsuda, J.L. Fox, W.I. Higuchi, Novel skeletal drug delivery system using self-setting calcium phosphate cement 9: effects of the mixing solution volume on anticancer drug-release from homogeneous drug-loaded cement, J. Pharm. Sci. 84 (6) (1995) 733–736.
[41] M. Bohner, J. Lemaitre, P. VanLanduyt, P.Y. Zambelli, H.P. Merkle, B. Gander, Gentamicin-loaded hydraulic calcium phosphate bone cement as antibiotic delivery system, J. Pharm. Sci. 86 (5) (1997) 565–572.
[42] M. Bohner, J. Lemaitre, H.P. Merckle, B. Gander, Control of gentamicin release from a calcium phosphate admixed poly(acrylic acid), J. Pharm. Sci. 89 (10) (2000) 1262–1270.
[43] T. Suzuki, K. Arai, H. Goto, M. Hanano, J. Watanabe, K. Tomono, Dissolution tests for self-setting calcium phosphate cement-containing nifedipine, Chem. Pharm. Bull. 50 (6) (2002) 741–743.
[44] B. Palazzo, M.C. Sidoti, N. Roveri, A. Tampieri, M. Sandri, L. Bertolazzi, F. Galbusera, G. Dubini, P. Vena, R. Contro, Controlled drug delivery from porous hydroxyapatite grafts: an experimental and theoretical approach, Mater. Sci. Eng. C25 (2005) 207–213.
[45] M. Vallet-Regi, A. Ramila, R.P. del Real, J. Perez-Pariente, A new property of MCM-41: drug delivery system, Chem. Mater. 13 (2) (2001) 308–311.
[46] P. Horcajada, A. Rámila, M. Gérard Férey, Vallet-Regí, Influence of superficial organic modification of MCM-41 matrices on drug delivery rate, Solid State Sci. 8 (2006) 1243–1249.
[47] Chaoyang Wang, Weihua Ye, Ying Zheng, Xinxing Liu, Zhen Tong, Fabrication of drug-loaded biodegradable microcapsules for controlled release by combination of solvent evaporation and layer-by-layer self-assembly, Int. J. Pharm. 338 (2007) 165–173.
[48] B. Narasimham, R. Langer, On the importance of the burst effect during drug release polymer films, Polym. Mater. Sci. Eng. Proc. 76 (1997) 558–569.
[49] D.M. Lin, S. Kalachandra, J. Valiyaparambil, S. Offenbacher, A polymeric device for delivery of anti-microbial and anti-fungal drugs in the oral environment: effect of temperature and medium on the rate of drug release, Dental Mater. 19 (7) (2003) 589–596.